

Full length article

Interfacial toughening effect of suture structures

Zengqian Liu^{a,b,*}, Zhefeng Zhang^{a,b,*}, Robert O. Ritchie^{c,**}^a Laboratory of Fatigue and Fracture for Materials, Institute of Metal Research, Chinese Academy of Sciences, Shenyang 110016, China^b School of Materials Science and Engineering, University of Science and Technology of China, Hefei 230026, China^c Department of Materials Science and Engineering, University of California Berkeley, Berkeley, CA 94720, USA

ARTICLE INFO

Article history:

Received 30 September 2019

Revised 2 November 2019

Accepted 15 November 2019

Available online 19 November 2019

Keywords:

Suture

Crack

Interface

Hierarchy

Toughening

ABSTRACT

Suture interfaces are one of the most common architectural designs in natural material-systems and are critical for ensuring multiple functionalities by providing flexibility while maintaining connectivity. Despite intensive studies on the mechanical role of suture structures, there is still a lack of understanding on the fracture mechanics of suture interfaces in terms of their interactions with impinging cracks. Here we reveal an interfacial toughening effect of suture structures by means of “excluding” cracks away from interfaces based on a dimensionless micro-mechanical model for single-leveled and hierarchical suture interfaces with triangular-shaped suture teeth. The effective stress-intensity driving forces for crack deflection along, versus penetration through, an interface at first impingement and on subsequent kinking are formulated and compared with the corresponding resistances. Quantitative criteria are established for discerning the cracking modes and fracture resistance of suture interfaces with their dependences on sutural tooth sharpness and interfacial toughness clarified. Additionally, the effects of structural hierarchy are elucidated through a consideration of hierarchical suture interfaces with fractal-like geometries. This study may offer guidance for designing bioinspired suture structures, especially for toughening materials where interfaces are a key weakness.

Statement of significance

Suture interfaces are one of the most common architectural material designs in biological systems, and are found in a wide range of species including armadillo osteoderms, boxfish armor, pangolin scales and insect cuticles. They are designed to provide flexibility while maintaining connectivity. Despite many studies on the mechanical role of suture structures, there is still little understanding of their role in terms of interactions with impinging cracks. Here we reveal an interfacial toughening effect of suture structures by means of “excluding” cracks away from interfaces based on a dimensionless micro-mechanical model for single-leveled and hierarchical suture interfaces with triangular-shaped suture teeth. Quantitative criteria are established for discerning the cracking mode and fracture resistance of the interfaces with their dependences on sutural tooth sharpness and interfacial toughness clarified.

© 2019 Acta Materialia Inc. Published by Elsevier Ltd. All rights reserved.

1. Introduction

Suture interfaces are one of the most common architectural designs of materials in biological systems which have evolved independently in a wide range of species [1–3]. Typical examples incorporating suture structures include the mammal crania [4–6],

woodpecker beak [7], armadillo osteoderms [8], turtle carapace [9,10], boxfish armor [11], pangolin scale [12,13], insect cuticle [14], seashells [15,16], diatoms [17], and seedcoats of succulents and grasses [18,19]. A suture interface is principally featured by the connection of generally stiff skeletal blocks or components via a compliant interfacial seam along geometrically complex boundaries, as shown in Fig. 1a,b. Specifically, the suture interfaces in some material-systems display a fractal-like hierarchical nature where higher-ordered structures of similar geometries, but with smaller dimensions, are superimposed onto lower-ordered ones [15,20] (Fig. 1b).

A major function of suture interfaces is to provide flexibility, while maintaining structural integrity, to accommodate respi-

* Corresponding authors at: Laboratory of Fatigue and Fracture for Materials, Institute of Metal Research, Chinese Academy of Sciences, Shenyang 110016, China.

** Corresponding author at: Department of Materials Science and Engineering, University of California Berkeley, Berkeley, CA 94720, USA.

E-mail addresses: zengqianliu@imr.ac.cn (Z. Liu), zhfzhang@imr.ac.cn (Z. Zhang), rortitche@lbl.gov (R.O. Ritchie).

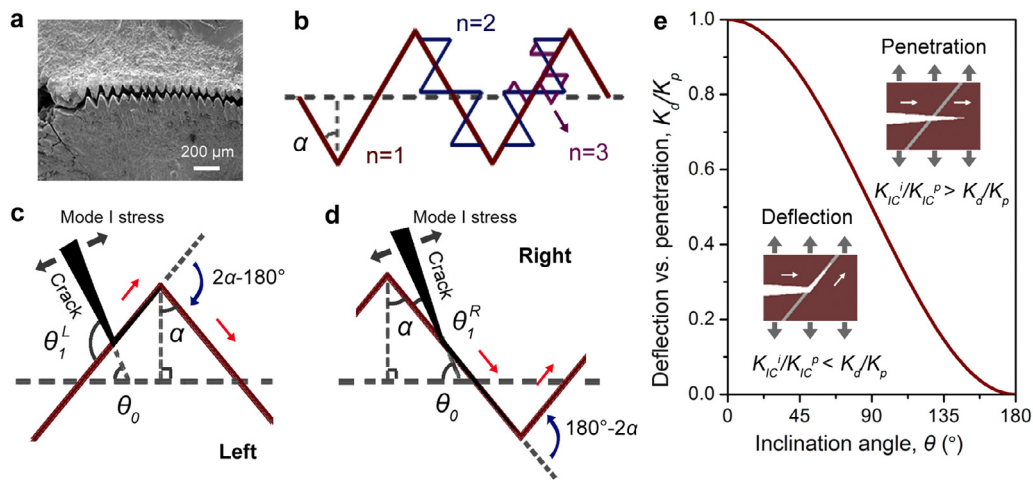


Fig. 1. Suture interface and its interaction with a crack. (a) Typical suture interface joining the scutes in boxfish armor [10]. (b) Schematic illustrations of triangular-shaped fractal-like suture interfaces with the levels of structural hierarchy up to 3. (c, d) Illustrations of the interactions between the crack and suture interface for crack impingement at the (c) left and (d) right sides of suture tooth. (e) Dependence of the ratio between the effective stress-intensity driving force for crack deflection and penetration, K_d/K_p , with the angle of crack inclination with respect to the interface, θ , for an originally pure mode I crack. The criteria for the two cracking modes are illustrated in the insets. (a) is adapted with permission from ref. [11].

ration, growth and locomotion of organisms without critically declining the stiffness and strength of materials [2,5,10,21,22]. Additionally, the suture interfaces that join brittle components can play an effective role in toughening materials by increasing the complexity of crack propagation via directing cracks into wavy paths [1–3,23–25]. The mechanical behavior of suture interfaces, including stiffness, strength and failure mechanisms, has been broadly explored in recent years [16,20,23–31]. Relationships have been established to correlate these properties with the geometrical parameters of the sutures, e.g., the shape, tip angle and width of the suture teeth, and the levels of structural hierarchy, together with the characteristics of the materials, e.g., the Young's moduli and fracture toughnesses of the skeletal components and interfacial seam. Moreover, the design principles of naturally-occurring suture structures have been increasingly implemented in the development of new bioinspired materials [23–25,28–30,32–34]. Such a strategy is particularly effective in toughening inherently brittle systems, such as glasses and ceramics [33,34].

Differing from hyper-mineralized materials like seashells, the skeletal components of suture structures in most of the less-mineralized biological systems are not brittle, but usually possess good combinations of strength and fracture toughness. This is particularly widespread in natural materials containing large amounts of collagens (e.g., mammal crania [4–6], turtle carapace [9,10] and boxfish armor [11]), keratins (e.g., woodpecker beak [7] and pangolin scale [12,13]) and chitins (e.g., insect cuticle [14]), and in plant systems [18,19]. However, the interfaces in these natural materials may provide prime sites of weakness as easy interfacial cracking can severely compromise their mechanical properties. From a perspective of structural integrity and the generation of superior damage tolerance, it is therefore preferable to confine the development of any crack within the skeletal components rather than channeling it into an interface. This contrasts with the scenario in hyper-mineralized biological materials and many brittle ceramics where interfacial or intergranular fracture can promote toughness [35–37]. Consequently, the question arises as to how the suture structure can affect the interactions between cracks and the interface, specifically in terms of determining the mode of crack advance. Indeed, despite the current consensus about the toughening effect of suture interfaces due to the “capture” of cracks in brittle systems [1–3,23–25], it remains unclear whether a suture structure may actually act in an opposite fashion to “exclude” cracks into the skeletal compo-

nents, particularly where the material is composed of less brittle constituents.

2. Theoretical considerations

Here we focus on the impingement of an originally straight crack under a pure mode I stress state onto a suture interface. Our approach is to explore the effects of sutural geometrical characteristics and structural hierarchy on the cracking mode by deflecting into, versus penetrating through, the interface. This issue is addressed by comparing the crack driving forces (i.e., the effective stress intensities) at a crack front with the corresponding fracture resistances (i.e., the fracture toughnesses of the interface and skeletal component). We consider a two-dimensional micro-mechanical model that is independent of length-scale or dimension, as illustrated in Fig. 1c,d; accordingly, the specific influence of remote interfaces and cracking paths on the stress state at the crack tip is not explicitly taken into account.

The suture teeth are considered to exhibit a triangular shape which is common in nature and has been proven to promote a uniform stress distribution among various geometries to allow for the high stiffness, strength and toughness of the material [23,26,27,32]. The skeletal components are presumed to be isotropically elastic and homogeneous to exclude the effects of plasticity and mechanical anisotropy. The suture structure is considered to be composed of the same material on both sides of interface. This is consistent with the fact that suture interfaces are most commonly formed between identical skeletal components in nature [4–19]. Additionally, the interface is presumed to be thin enough such that the direction of any interfacial cracking conforms exactly to the interfacial profile (without considering additional crack deflection within the interface). This assumption is reasonable as most suture interfaces in biological materials exhibit a limited thickness, especially as compared to the dimension of their skeletal components. For example, the thicknesses of the suture interfaces in armadillo osteoderms and boxfish armor are, respectively, $\sim 1/20$ and $1/200$ of the widths of the osteoderm scales and boxfish scutes [8,11]. Similarly, the epidermis cells constituting *Panicum miliaceum* and *Portulaca oleracea* seedcoats are over 20 times larger than the interfacial thicknesses of their suture structures [18,19].

The strength of a suture interface has been elucidated in terms of the competition between interfacial shear and normal failure of the suture tooth [26]. Nevertheless, in the presence of

cracks it is the fracture toughness that plays the dominant role in determining the cracking mode and fracture resistance. Here the fracture toughnesses of the interface and the skeletal component, represented respectively by the critical mode I stress intensities, K_{IC}^i and K_{IC}^b , are presumed to be constant. These stress intensities can provide a direct assessment of the intrinsic resistance to cracking within the two phases.

A crack may continue to extend when impinging on an interface in two principal modes, specifically, deflection (or kinking) into, versus penetration through, the interface [33,38–43]. The competition between these modes is determined by their energy release rates or effective stress intensities for cracking which are closely dependent on the inclination angle between the crack and the interface. Here the inclination angle is defined to be positive by counterclockwise rotation from the crack wake to the interface. Similarly, the deflection (or kinking) angle of the crack is defined to be positive in counterclockwise fashion. With respect to crack kinking at an angle θ , the crack tip will be subjected to both tensile and shear stresses despite the pure mode I stress state of the far-field loading. The mode I and mode II stress intensities, K_I and K_{II} , for an infinitely-small and kinked crack, i.e., at the onset of crack kinking, can be expressed respectively as [35,40,43]:

$$K_I = C_{11}(\theta)k_I + C_{12}(\theta)k_{II} \tag{1}$$

and

$$K_{II} = C_{21}(\theta)k_I + C_{22}(\theta)k_{II}, \tag{2}$$

where

$$C_{11}(\theta) = \cos^3(\theta/2),$$

$$C_{12}(\theta) = -3 \sin(\theta/2)\cos^2(\theta/2),$$

$$C_{21}(\theta) = \sin(\theta/2)\cos^2(\theta/2),$$

$$C_{22}(\theta) = \cos(\theta/2)[1 - 3\sin^2(\theta/2)].$$

k_I and k_{II} are the stress intensities for the initial incident crack, with $k_{II} = 0$ in case of an originally pure mode I stress state before kinking.

The effective stress intensities for crack deflection (or kinking) into the interface, K_d , and for crack penetration through the interface, K_p , can be obtained as:

$$K_d = (K_I^2 + K_{II}^2)^{1/2} = k_I \cos^2(\theta/2), \tag{3}$$

and

$$K_p = (k_I^2 + k_{II}^2)^{1/2} = k_I. \tag{4}$$

K_d and K_p represent the driving forces for the two cracking modes exerted by the applied load. The competition between crack deflection and penetration can be evaluated by comparing these driving forces with the corresponding resistances, as follows [33]:

$$K_d/K_p = \cos^2(\theta/2) > K_{IC}^i/K_{IC}^b \text{ (deflection)}, \tag{5}$$

and

$$K_d/K_p = \cos^2(\theta/2) < K_{IC}^i/K_{IC}^b \text{ (penetration)}, \tag{6}$$

where K_{IC}^i and K_{IC}^b are the critical stress intensities (i.e., fracture toughness values) of the interface and bulk component, respectively.

The inclination angle of the crack with respect to the interface plays a critical role in determining the effective stress-intensity driving force for crack deflection versus penetration, thereby dictating the cracking mode at the first impingement. For a given interfacial toughness normalized to that of the skeletal component K_{IC}^i/K_{IC}^b , the crack tends to penetrate through the interface when the inclination angle is larger than a critical value, otherwise it will deflect into interface, as shown in Fig. 1e. This critical angle

decreases monotonically from 180° to 0° as the normalized interfacial toughness increases from 0 (i.e., the interface approximates an open crack) to 1 (or equivalently without interface). It is noted that when θ exceeds 90°, it may be easier for a crack to kink by a supplementary angle of θ . This is taken into account here by considering crack kinking only to the right side but examining an entire range of initial incident angles from 0° to 180° in view of the geometrical symmetry (Fig. 1c,d).

3. Results

3.1. Interaction of crack with the suture interface

We now analyze the interaction of a crack with the suture interface where the apex angle of the triangular-shaped suture tooth is 2α , with α defined as the sutural tip angle as illustrated in Fig. 1c,d. The crack may impinge onto the interface at both sides of the suture tooth. The actual inclination angles for impingement at the left side and right side, θ_1^L and θ_1^R , can be determined as a function of the sutural tip angle as:

$$\theta_1^L = \theta_0 + 90^\circ - \alpha \tag{7}$$

and

$$\theta_1^R = \theta_0 - 90^\circ + \alpha, \tag{8}$$

respectively, where θ_0 is the initial incident angle of the crack with respect to an originally straight interface without a suture structure.

In the case of a left-side impingement, the actual inclination angle θ_1^L is invariably larger than θ_0 , leading to a decrease in the effective stress intensity for crack deflection relative to penetration, as compared to a suture-free interface (Fig. 1e). This implies an improved propensity for crack penetration through the interface for given cracking resistances of the interface and skeletal component. As such, interfacial cracking can be retarded even though the real toughness of the interface remains constant, suggesting an interfacial toughening effect. Nevertheless, the suture structure results in a decreased inclination angle θ_1^R than θ_0 when the crack impinges at the right side of the suture tooth. This makes the crack more easily “captured” in the interface by increasing the effective stress intensity for crack deflection versus penetration (Fig. 1e).

Therefore, at the first impingement, the suture structure does not necessarily act to toughen the interface, but may also promote interfacial cracking in terms of the kinking of incident cracks into the interface. For the latter case, however, subsequent propagation of the interfacial crack necessitates a constant crack deflection along the zig-zag profile of suture interface, i.e., crack kinking should always prevail over penetration into the skeletal component. Next, we explore the advance of a kinked crack with its front approaching the tip of the suture tooth. The crack may penetrate through the interface or continuously deflect along it; the latter represents a second kinking of an oblique crack which has been kinked by an angle θ (i.e., θ_1^L or θ_1^R) with respect to its originally pure mode I direction. The mode I and mode II stress intensities for a singly-kinked crack can be approximated using K_I and K_{II} provided there is a limited kinking length compared to the main crack [40,43]. For an infinitely small crack tip which is additionally kinked by angle φ , the stress intensities K_I' and K_{II}' at the crack tip can be obtained by substituting K_I and K_{II} into Eqs. (1) and (2) for k_I and k_{II} as:

$$\begin{aligned} K_I' &= C_{11}(\varphi)K_I + C_{12}(\varphi)K_{II} \\ &= k_I[\cos^3(\theta/2)\cos^3(\varphi/2) \\ &\quad - 3 \sin(\theta/2)\cos^2(\theta/2) \sin(\varphi/2)\cos^2(\varphi/2)], \end{aligned} \tag{9}$$

and

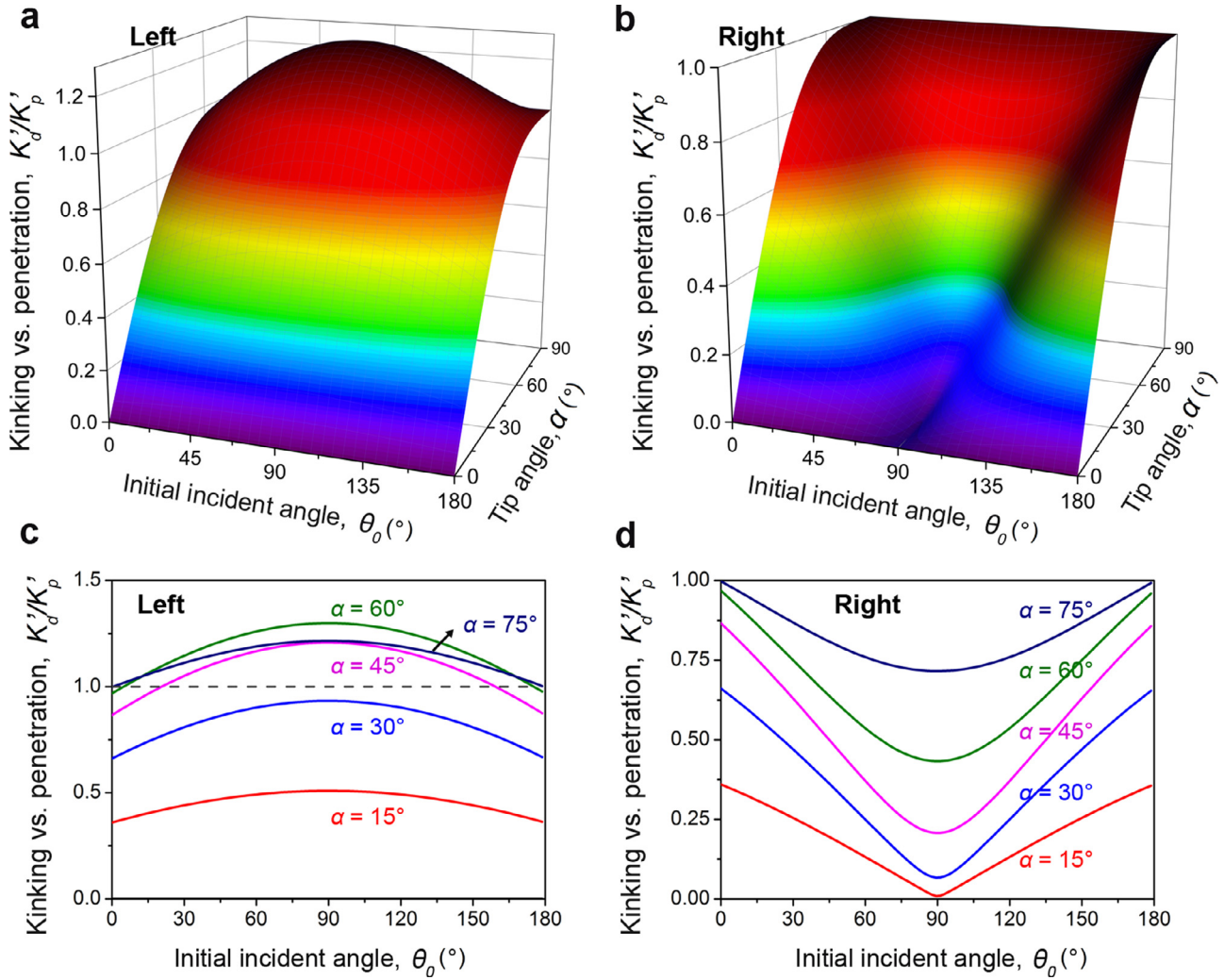


Fig. 2. Driving forces for second crack kinking versus penetration. (a, b) Dependences of the ratio between the effective stress intensities for second kinking and penetration, K'_d/K'_p , for a crack approaching the tip of a suture tooth at an initial incident angle θ_0 and sutural tip angle α when the first impingement occurs at the (a) left and (b) right sides of the suture tooth. (c, d) Variations in K'_d/K'_p as a function of θ_0 over the entire incident range of specific sutural tip angles with α at 15°, 30°, 45°, 60° and 75° for case of the first impingement at the (c) left and (d) right sides of the suture tooth.

$$K'_{II} = C_{21}(\varphi)K_I + C_{22}(\varphi)K_{II} = k_I \{ \sin(\varphi/2) \cos^2(\varphi/2) \cos^3(\theta/2) + \sin(\theta/2) \cos^2(\theta/2) \cos(\varphi/2) [1 - 3\sin^2(\varphi/2)] \}. \quad (10)$$

The effective stress intensity for the second kinking of the crack, K'_d , can thus be obtained as:

$$K'_d = (K_I'^2 + K_{II}^2)^{1/2} = k_I \cos^2(\theta/2) [\cos^4(\varphi/2) + 4\sin^2(\varphi/2) \cos^2(\varphi/2) \sin^2(\theta/2) - 4\sin(\varphi/2) \cos^3(\varphi/2) \sin(\theta/2) \cos(\theta/2)]^{1/2}. \quad (11)$$

The effective stress intensity for crack penetration into the skeletal component, K'_p , can be approximated using that for the crack kinking at first impingement with the interface as:

$$K'_p = K_d = (K_I^2 + K_{II}^2)^{1/2} = k_I \cos^2(\theta/2). \quad (12)$$

As such, the ratio between the effective stress-intensity driving forces for second crack kinking and penetration at the tip of the suture tooth can be described as a function of the kinking angles θ and φ as:

$$K'_d/K'_p = [\cos^4(\varphi/2) + 4\sin^2(\varphi/2) \cos^2(\varphi/2) \sin^2(\theta/2) - 4\sin(\varphi/2) \cos^3(\varphi/2) \sin(\theta/2) \cos(\theta/2)]^{1/2}. \quad (13)$$

The cracking mode can thus be determined by comparing driving forces with corresponding resistances as:

$$K'_d/K'_p > K_{IC}^i/K_{IC}^b \text{ (deflection)}, \quad (14)$$

and

$$K'_d/K'_p < K_{IC}^i/K_{IC}^b \text{ (penetration)}. \quad (15)$$

As illustrated in Fig. 1c and d, the kinking angles (θ , φ) are $(\theta_1^L, 2\alpha - 180^\circ)$ and $(\theta_1^R, 180^\circ - 2\alpha)$, respectively, when the first impingement occurs at the left and right sides of suture tooth. In both situations, the ratio of the effective stress intensities K'_d/K'_p for cracks with an initial incident angle θ_0 ranging from 0° to 180° can be obtained by combining Eqs. (7), (8) and (13), as shown in Fig. 2a,b. The variations in K'_d/K'_p with θ_0 for specific sutural tip angles with α set at 15°, 30°, 45°, 60° and 75° are shown in Fig. 2c,d. It is seen that for left-side impingement, the introduction of relatively sharp suture structures (e.g., α is 15° or 30°) leads to smaller K'_d/K'_p over the entire incident range compared to the case for a suture-free straight interface (i.e., with $K'_d/K'_p = 1$ as denoted by dashed line) (Fig. 2a and c). Consequently, cracks become more prone to penetrate through the interface and propagate into the skeletal component for a given interfacial toughness. Nevertheless, K'_d/K'_p may be larger than unity when the suture tooth is relatively

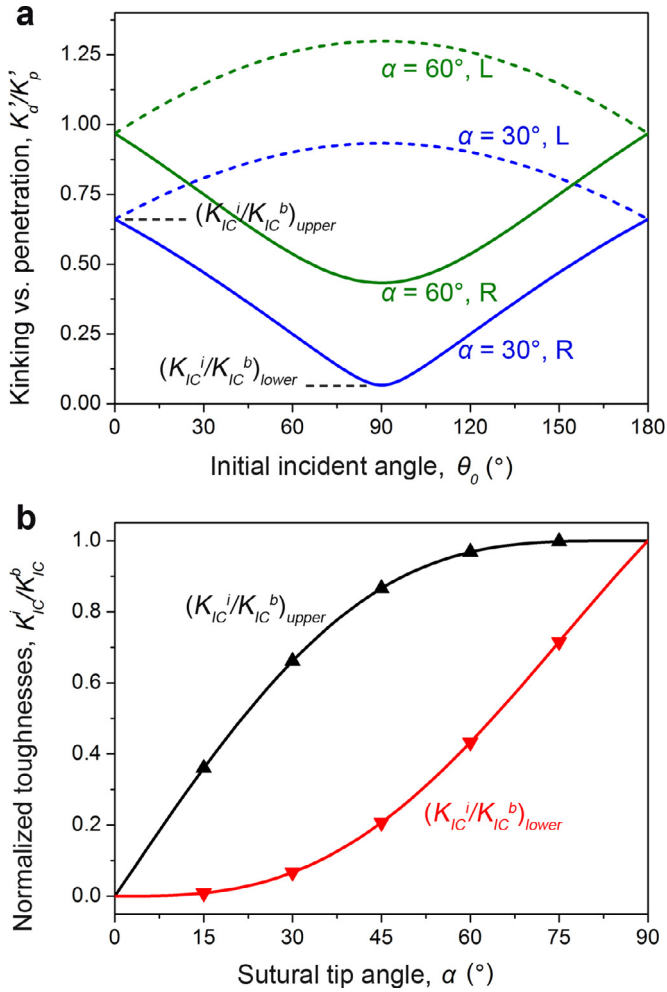


Fig. 3. Characteristic interfacial toughnesses and effects of sutural tooth sharpness. (a) Definition of the characteristic interfacial toughnesses normalized by those of the skeletal components, $(K'_{IC}/K'_{IC})_{lower}$ and $(K'_{IC}/K'_{IC})_{upper}$, by comparing the ratios between the effective stress-intensities for second crack kinking and penetration, K'_d/K'_p , in the case of left- (L) and right-side (R) impingements for specific sutural tip angles with α at 30° and 60° . (b) Variations in $(K'_{IC}/K'_{IC})_{lower}$ and $(K'_{IC}/K'_{IC})_{upper}$ as a function of the sutural tip angle α for a single-leveled suture interface.

obtuse (e.g., α is 45° , 60° or 75°), implying easier crack deflection along interface by a second kinking (compared to the case for suture-free interface). In comparison, cracks invariably exhibit a smaller K'_d/K'_p below unity because of the presence of suture structures for the case of the first impingement occurring at the right side of the suture tooth (Fig. 2b and d). This leads to an interfacial toughening effect by resisting further crack advance along the interface. Such an effect can be increasingly enhanced, as indicated by the decrease in K'_d/K'_p , as the suture tooth becomes sharpened with decreasing sutural tip angle.

Additionally, for a given sutural tip angle, cracks will display a smaller K'_d/K'_p for all initial incident angles when the first impingement occurs at the right side of the suture tooth compared to the case for the left side, as shown in Fig. 3a. This makes the second kinking of the crack, in the form of “right-to-left” side on the suture tooth, a key step in determining whether a crack can constantly deflect along the interface. The prevalence of such crack kinking over penetration will lead to continuous interfacial cracking by enabling successive deflection. Otherwise, the crack will be eventually excluded away from the interface into the skeletal component even though crack kinking with other configurations

(e.g., from left to right side on the suture tooth for a single-leveled suture interface) may be preferred.

For an improved description of these interactions between cracks and the suture interface, we can define two characteristic values for the interfacial toughness normalized by that of the bulk component, $(K'_{IC}/K'_{IC})_{lower}$ and $(K'_{IC}/K'_{IC})_{upper}$, as indicated in Fig. 3a. $(K'_{IC}/K'_{IC})_{lower}$ denotes the minimum of the effective stress-intensity ratios for crack deflection versus penetration K'_d/K'_p for all modes of double kinking (i.e., with first impingement at both left and right sides of the suture tooth) over the entire initial incident range. Any crack advance will be confined into the interface when the normalized interfacial toughness is lower than $(K'_{IC}/K'_{IC})_{lower}$. $(K'_{IC}/K'_{IC})_{upper}$ is defined as the maximum value of the lower-bound K'_d/K'_p over the entire incident range which corresponds to relatively difficult modes of double kinking (i.e., right-side impingement in case of single-leveled suture structure). Any crack will eventually propagate into the skeletal component by penetrating through the interface when the normalized interfacial toughness is higher than $(K'_{IC}/K'_{IC})_{upper}$. For a single-leveled suture interface, $(K'_{IC}/K'_{IC})_{lower}$ and $(K'_{IC}/K'_{IC})_{upper}$ can be determined as a function of the sutural tip angle as:

$$(K'_{IC}/K'_{IC})_{lower} = [\sin^4\alpha + 4\sin^2\alpha\cos^2\alpha\sin^2(\alpha/2) - 2\sin^4\alpha\cos\alpha]^{1/2}, \quad (16)$$

and

$$(K'_{IC}/K'_{IC})_{upper} = \{\sin^4\alpha + 4\sin^2\alpha\cos^2\alpha\sin^2[(\alpha - 90^\circ)/2] + 2\sin^3\alpha\cos^2\alpha\}^{1/2}. \quad (17)$$

As shown in Fig. 3b, both $(K'_{IC}/K'_{IC})_{lower}$ and $(K'_{IC}/K'_{IC})_{upper}$ are lowered by the presence of a suture structure to a value below unity which corresponds to a suture-free straight interface (i.e., with $\alpha = 90^\circ$). These parameters exhibit a monotonically decreasing trend as the suture tooth becomes increasingly sharpened (i.e., with decreasing α). This indicates that by inhibiting crack advance along the interface, the suture structure plays an interfacial toughening role which is positively related to the sharpness of the suture tooth. Taking $\alpha = 15^\circ$ for example, the constant deflection of all cracks along the interface necessitates an extremely weak interface with a toughness lower than 0.9% of that for the bulk component. Moreover, any interfacial cracking can be eventually impeded as long as the interface is not more than 64% less tough than that of the skeletal component. Such a toughening efficiency is remarkable considering that, in the absence of a suture structure, a similar result can only be achieved when the interface is as tough as the component itself. The above theoretical findings are consistent with the results from finite element simulations on suture interfaces with differing degrees of waviness [23,27,30,44]. It has been shown that crack propagation along a suture interface can be effectively retarded as the waviness of the interfacial layer increases (i.e., the sutural tip angle decreases), leading to an improved fracture toughness of the entire structure. This has also been validated by experiments using bioinspired polymer prototypes with designed sutural geometries manufactured by a 3-D printing technique [23,30,44].

3.2. Effects of structural hierarchy

In the following, we explore the effects of structural hierarchy by examining the interactions between cracks and a hierarchical suture interface with fractal-like geometries. The suture teeth at each level of hierarchy are taken to be triangular in shape with the same sutural tip angle of α (Fig. 1b). As illustrated in Fig. 1c and d, the actual inclination angle of the crack with respect to

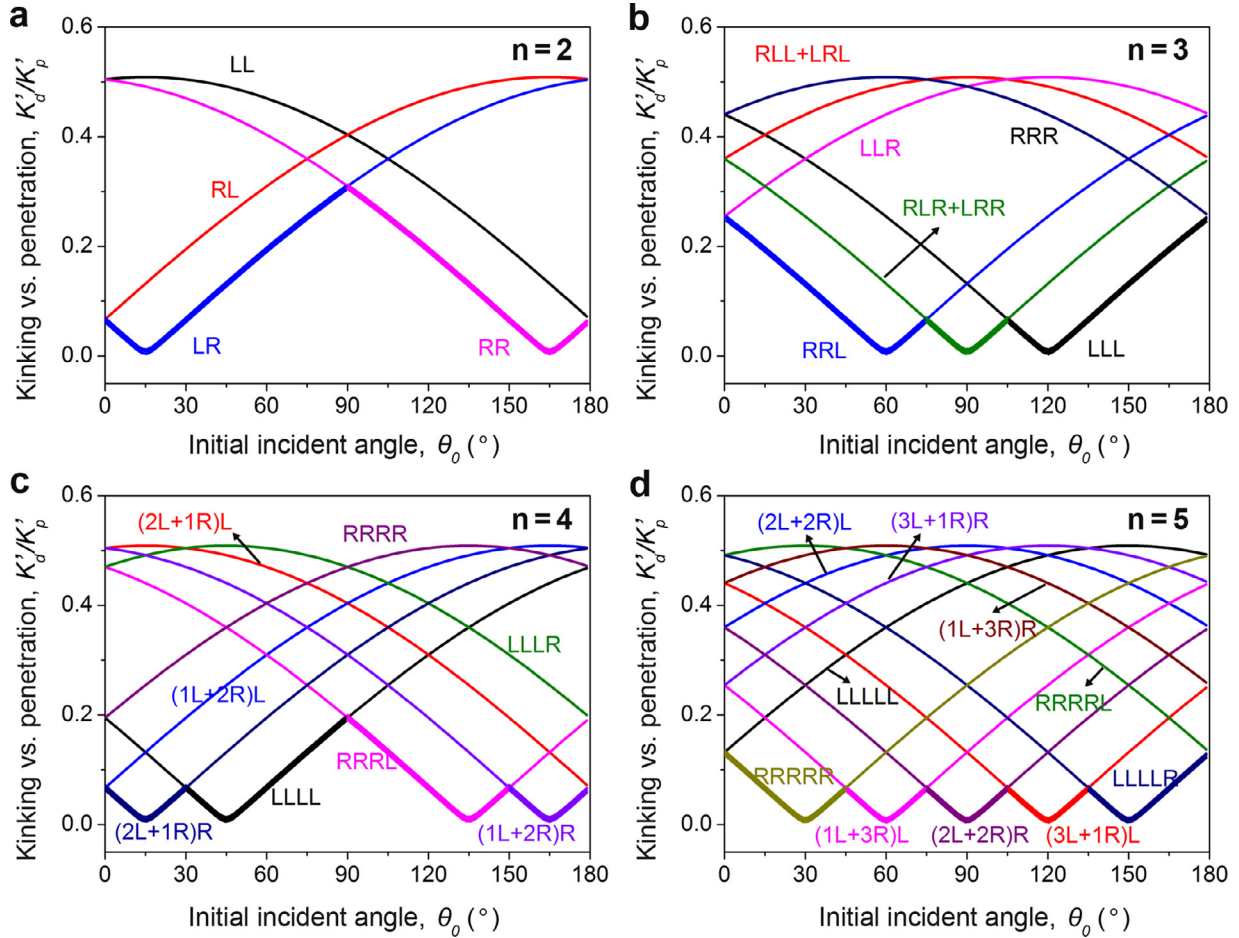


Fig. 4. Crack kinking versus penetration for hierarchical suture interfaces. Variations in the ratio between the effective stress intensities for second crack kinking and penetration, K'_d/K'_p , over the entire range of initial incident angles θ_0 for fractal-like hierarchical suture interfaces having (a) 2, (b) 3, (c) 4, and (d) 5 levels of structural hierarchy and specific sutural tip angle with $\alpha = 15^\circ$. The detailed modes for the double kinking of cracks are indicated by the position of the crack impingement on the suture teeth with the letters R and L representing “right” and “left”. The level of structural hierarchy is denoted by the number of letters. For example, “RRL” indicates that the crack impinges onto the left side of the finest suture tooth for a suture structure with 3 levels of hierarchy. The 3-ordered suture tooth locates at the right side of the 2-ordered one which additionally locates at the right side of the primary suture tooth. Competition between second crack kinking and penetration for other sutural tip angles, with α at 30° , 45° , 60° and 75° , are shown in Figs. S1–S4 in the Supplementary Materials.

the interface at n -ordered hierarchy can be correlated to that for a lower-ordered structural level in a similar fashion with Eqs. (7) and (8) as:

$$\theta_n^L = \theta_{n-1} + 90^\circ - \alpha \quad (18)$$

and

$$\theta_n^R = \theta_{n-1} - 90^\circ + \alpha, \quad (19)$$

where the superscripts L and R denote that the impingement occurs at the left and right sides of the finest suture tooth. The inclination angle at the $n - 1$ level of hierarchy, θ_{n-1} , has a couple of possibilities, specifically θ_{n-1}^L or θ_{n-1}^R , considering that the higher-ordered suture teeth may be located at either the left or right side of the lower-ordered ones. As such, the number of modes for crack-interface intersections can be doubled with each increase in structural hierarchy, giving 2^n possibilities for n -ordered suture interface.

With respect to the second kinking of deflected cracks, the kinking angles equal those for the single-leveled suture structure as $2\alpha - 180^\circ$ and $180^\circ - 2\alpha$, respectively, when the crack impinges at the left and right sides of the highest-ordered suture tooth. Therefore, the ratio between the effective stress intensities for crack deflection and penetration at the tip of the suture tooth, K'_d/K'_p , can be obtained according to Eq. (13) by substituting the

kinking angles (θ , φ) using $(\theta_n^L, 2\alpha - 180^\circ)$ and $(\theta_n^R, 180^\circ - 2\alpha)$, respectively, for left- and right-side impingement of a crack with the finest suture tooth.

Fig. 4 shows the variations in K'_d/K'_p over the entire range of initial incident angles θ_0 for cracks intersecting with hierarchical suture interfaces which have a specific sutural tip angle with $\alpha = 15^\circ$ and display differing structural hierarchies up to 5. The cases for other sutural geometries with α equal to 30° , 45° , 60° and 75° are plotted in Figs. S1–S4 in the Supplementary Materials. The detailed modes for double kinking are indicated by the position of first crack impingement. For example, for the interaction of a crack with a suture interface having 2 levels of hierarchy, “RL” denotes that the second kinking originates from a first impingement on the left side of a 2-ordered suture tooth which is located at the right side of the primary tooth. It is shown that the increase in structural hierarchy leads to a multiplicity of kinking modes for the crack in terms of the competition between crack deflection and penetration (some of these modes may be equivalent for second kinking as indicated by the overlap of K'_d/K'_p curves). To maintain constant crack deflection along the interface, crack kinking should always prevail over penetration for all of these modes. Otherwise, the crack will eventually be excluded away from the interface as long as crack kinking with the lowest propensity (*i.e.*, smallest K'_d/K'_p) is inhibited. Therefore, whether a

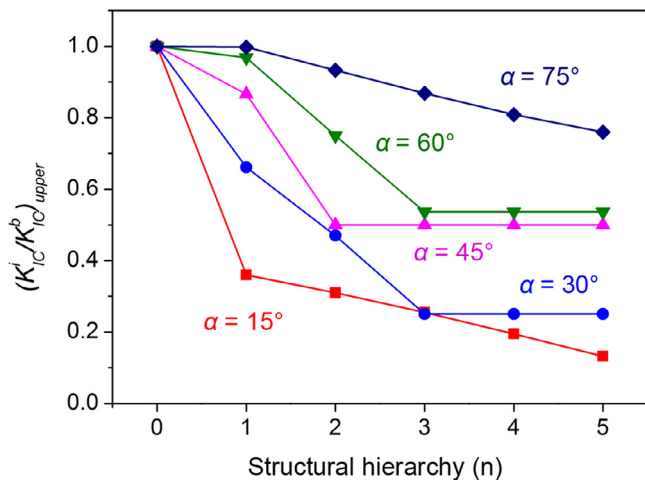


Fig. 5. Effects of structural hierarchy on the fracture resistance of suture interfaces. Dependences of the characteristic interfacial toughness normalized by that of the skeletal component $(K_{IC}^i/K_{IC}^b)_{upper}$ on the number of levels of structural hierarchy for fractal-like hierarchical suture interfaces which possess triangular-shaped suture teeth with specific sutural tip angles of α as 15° , 30° , 45° , 60° , and 75° .

crack may extend along suture interfaces with differing structural hierarchies is essentially determined by the lower bounds of K_d^i/K_p^b , as highlighted by the thick curves in Fig. 4.

It can be seen that the parameter $(K_{IC}^i/K_{IC}^b)_{lower}$ is independent of the levels of structural hierarchical for given sutural tip angles (Fig. 4 and Figs. S1–S4 in the Supplementary Materials). As such, the critical conditions for interfacial toughnesses remain constant in order to ensure the confinement of all incident cracks into the interfaces. Nevertheless, such characteristic values tend to appear at more initial incident angles as the number of hierarchical levels increases. This implies that cracks with broader initial incident ranges become more prone to penetrate through the interface when the normalized interfacial toughness is higher than $(K_{IC}^i/K_{IC}^b)_{lower}$.

On the other hand, the parameter $(K_{IC}^i/K_{IC}^b)_{upper}$, as the maximum of the lower bounds for K_d^i/K_p^b over the entire incident range, exhibits a generally decreasing trend with an increase in hierarchical levels, as shown in Fig. 5. Specifically, $(K_{IC}^i/K_{IC}^b)_{upper}$ may become stable over specific hierarchies for suture interfaces with right-angled teeth or close geometries (e.g., α is 30° , 45° , or 60°). Additionally, for a given level of hierarchy $(K_{IC}^i/K_{IC}^b)_{upper}$ tends to be decreased as the suture tooth becomes sharper (i.e., with decreasing α). Therefore, interfacial cracking can be increasingly retarded by the suture structure either by increasing the levels of structural hierarchy or by increasing the sharpness of the suture tooth. This plays a role in toughening the interface by shielding it from the applied stress even though the intrinsic interfacial toughness remains constant. For example, with respect to 5-ordered hierarchical suture interfaces encompassing relatively obtuse and sharp teeth with α as 75° and 15° , all incident cracks will eventually be excluded from the interface into the skeletal component as long as the interfacial toughnesses are not lower than 76% and 13%, respectively, of the corresponding toughness of the skeletal component. The analytical model proposed by Li et al. predicts a similar trend of increasing fracture toughness with the increase in structural hierarchy for fractal-like hierarchical suture structures [20,30]. This has also been experimentally validated by mechanical characterization of 3-D printed suture structures with differing structural hierarchies and complex geometries [32]. The enhanced toughness gained through increasing hierarchy was found to be associated with the generation of more “graceful” failure mechanisms that promoted energy dissipation by the suture joints.

4. Discussion

We note that suture interfaces in nature exhibit certain thicknesses and are filled with material which is more compliant or viscoelastic than the skeletal component. Nevertheless, neither the plastic deformation nor the structural or mechanical anisotropy of the constituents (either the interfacial seam or skeletal component) are considered in our analysis. Also, extrinsic toughening mechanisms, which mainly act behind a crack tip and are common in many biological materials, are also not taken into account [45,46]. Admittedly, plastic and viscoelastic deformation can play a major role in conferring compliance and in toughening the constituents [20,25,29], but these effects can always be integrated into the current model in terms of improvements in the intrinsic fracture toughnesses of the constituents (i.e., K_{IC}^i and K_{IC}^b). Indeed, plasticity represents a prime contribution to intrinsic toughening which acts to enhance the inherent resistance to cracking of a material instead of shielding the crack tip from the applied stresses [45,46]. The assumptions made here are formulated for elastic fracture mechanics (in terms of stress-intensity factors), which in terms of general trends we believe are pertinent to natural biological materials and 3-D printed suture structures where plasticity may be involved [8,11,20,23,44]. Additionally, the present model is presumed to be applicable to realistic suture interfaces as they usually comprise the same skeletal components on both sides and exhibit a limited interfacial thickness relative to the dimensions of the components.

Moreover, by examining a sufficiently large incident crack of a length considerably exceeding the characteristic dimension of a suture tooth, any kinking length for crack deflection along the interface can be regarded as infinitely small as compared to the originally pure mode I crack. The influence from any remote cracking paths and interfaces on the stress states can be additionally excluded by focusing on the tip region of the thin crack front. Therefore, the stress intensities derived for double kinking of cracks are also approximately applicable to those for multiple crack kinking or deflection, regardless of the cracking configurations along the interface [33,43,47,48]. This means that interfacial cracks approaching sutural tips are not necessarily kinked from a first impingement, but may have kinked by more times or even penetrated through several interfaces or suture teeth before being subjected to final kinking. Therefore, the current analysis can be employed to examine the competition for the kinking of a crack along, versus penetration through, the suture interface at any time. With such a scenario, this study may offer the basic means for discerning the crack-interface interactions and for evaluating the fracture resistance of suture structures.

5. Conclusions

By focusing on the crack-tip region based on a micro-mechanical model, we investigated the interaction of an impinging crack with a suture interface in terms of further crack advance by kinking along, versus penetration through, the interface. Criteria are established by exploring the driving forces of effective stress intensities for the two cracking modes - kinking vs. penetration - and comparing them with the corresponding resistances for the first impingement and for subsequent kinking at the tips of the suture teeth. Two characteristic parameters are proposed for the interfacial toughnesses in assessing whether a crack may constantly deflect along an interface. We reveal that the suture interface provides for interfacial toughening by resisting continuous crack kinking and promoting crack penetration through the interface into the skeletal component. Such an effect is positively correlated with the levels of structural hierarchy and the sharpness of the sutural tooth geometry. The increased propensity for “excluding” cracks away from an interface differs from the

general motif of “capturing” cracks by confining them within a weak interface, which is effective in toughening inherently brittle materials. Nevertheless, the inhibition of easy interfacial cracking and the direction of cracks into tough components by the presence of the suture interface should be more favorable for enhancing the fracture resistance of less-brittle materials which are widespread in nature. This study may aid the understanding of the mechanical role of naturally-occurring suture interfaces and offer guidance for designing bioinspired suture structures in man-made systems.

Declaration of Competing Interest

The authors declare that they have no known competing financial interests or personal relationships that could have appeared to influence the work reported in this paper.

Acknowledgements

The authors are grateful for the financial support by the National Natural Science Foundation of China under grant nos. 51871216 and 51331007 (for Z.L. and Z.Z.), and from the Multi-University Research Initiative under grant no. AFOSR-FA9550-15-1-0009 from the Air Force Office of Scientific Research to the University of California Riverside, specifically through a subcontract to the University of California Berkeley (for R.O.R.). Z.L. devotes this work to his little son, Jinlu, who is particularly good at laughing.

Supplementary materials

Supplementary material associated with this article can be found, in the online version, at doi:10.1016/j.actbio.2019.11.034.

References

- [1] F. Barthelat, Z. Yin, M.J. Buehler, Structure and mechanics of interfacial biological materials, *Nat. Rev. Mater.* 1 (2016) 1–16.
- [2] P. Fratzl, O. Kolednik, F.D. Fischer, M.N. Dean, The mechanics of tessellations – bioinspired strategies for fracture resistance, *Chem. Soc. Rev.* 45 (2016) 252–267.
- [3] S.E. Naleway, M.M. Porter, J. McKittrick, M.A. Meyers, Structural design elements in biological materials: application to bioinspiration, *Adv. Mater.* 27 (2015) 5455–5476.
- [4] S.M. Warren, L.J. Brunet, R.M. Harland, A.N. Economides, M.T. Longaker, The BMP antagonist noggin regulates cranial suture fusion, *Nature* 422 (2003) 625–629.
- [5] C.R. Jaslow, A.A. Biewener, Strain patterns in the horncores, cranial bones and sutures of goats (*Capra hircus*) during impact loading, *J. Zool.* 235 (1995) 193–210.
- [6] C.W. Nicolay, M.J. Vaders, Cranial suture complexity in white-tailed deer (*Odocoileus virginianus*), *J. Morphol.* 267 (2006) 841–849.
- [7] N. Lee, M.F. Horstemeyer, H. Rhee, B. Nabors, J. Liao, L.N. Williams, Hierarchical multiscale structure-property relationships of the red-bellied woodpecker (*Melanerpes carolinus*) beak, *J. R. Soc. Interface* 11 (2014) 20140274.
- [8] I.H. Chen, J.H. Kiang, V. Correa, M.I. Lopez, P.Y. Chen, J. McKittrick, M.A. Meyers, Armadillo armor: mechanical testing and micro-structural evaluation, *J. Mech. Behav. Biomed. Mater.* 4 (2011) 713–722.
- [9] B. Achrai, H.D. Wagner, Micro-structure and mechanical properties of the turtle carapace as a biological composite shield, *Acta Biomater.* 9 (2013) 5890–5902.
- [10] S. Krauss, E. Monsonogo-Orman, E. Zelzer, P. Fratzl, R. Shahar, Mechanical function of a complex three-dimensional suture joining the bony elements in the shell of the red-eared slider turtle, *Adv. Mater.* 21 (2009) 407–412.
- [11] W. Yang, S.E. Naleway, M.M. Porter, M.A. Meyers, J. McKittrick, The armored carapace of the boxfish, *Acta Biomater.* 23 (2015) 1–10.
- [12] B. Wang, W. Yang, V.R. Sherman, M.A. Meyers, Pangolin armor: overlapping, structure, and mechanical properties of the keratinous scales, *Acta Biomater.* 41 (2016) 60–74.
- [13] Z.Q. Liu, D. Jiao, Z.Y. Weng, Z.F. Zhang, Structure and mechanical behaviors of protective armored pangolin scales and effects of hydration and orientation, *J. Mech. Behav. Biomed. Mater.* 56 (2016) 165–174.
- [14] J.F.V. Vincent, U.G.K. Wegst, Design and mechanical properties of insect cuticle, *Arthropod Struct. Dev.* 33 (2004) 187–199.
- [15] W.B. Saunders, D.M. Work, S.V. Nikolaeva, Evolution of complexity in Paleozoic ammonoid sutures, *Science* 286 (1999) 760–763.
- [16] F. Barthelat, H. Tang, P.D. Zavattieri, C.M. Li, H.D. Espinosa, On the mechanics of mother-of-pearl: a key feature in the material hierarchical structure, *J. Mech. Phys. Solids* 55 (2007) 306–337.
- [17] K.M. Manoylov, N. Ognjanova-Rumenova, R.J. Stevenson, Morphotype variations in subfossil diatom species of Aulacoseira in 24 Michigan Lakes, USA, *Acta Bot. Croat* 68 (2009) 401–419.
- [18] B.P.J. Hasseldine, C. Gao, J.M. Collins, H.D. Jung, T.S. Jang, J. Song, Y. Li, Mechanical response of common millet (*Panicum miliaceum*) seeds under quasi-static compression: experiments and modeling, *J. Mech. Behav. Biomed. Mater.* 73 (2017) 102–113.
- [19] C. Gao, H.P.J. Hasseldine, L. Li, J.C. Weaver, Y. Li, Amplifying strength, toughness, and auxeticity via wavy sutural tessellation in plant seedcoats, *Adv. Mater.* 30 (2018) 1800579.
- [20] Y. Li, C. Ortiz, M.C. Boyce, Bioinspired, mechanical, deterministic fractal model for hierarchical suture joints, *Phys. Rev. E* 85 (2012) 031901.
- [21] R.P. Hubbard, J.W. Melvin, I.T. Barodawala, Flexure of cranial sutures, *J. Biomech.* 4 (1971) 491–492.
- [22] S.W. Herring, Mechanical influences on suture development and patency, *Front. Oral Biol.* 12 (2008) 41–56.
- [23] E. Lin, Y. Li, C. Ortiz, M.C. Boyce, 3D printed, bio-inspired prototypes and analytical models for structured suture interfaces with geometrically-tuned deformation and failure behavior, *J. Mech. Phys. Solids* 73 (2014) 166–182.
- [24] F.A. Cordisco, P.D. Zavattieri, L.G. Hector Jr., A.F. Bower, Toughness of a patterned interface between two elastically dissimilar solids, *Eng. Fract. Mech.* 96 (2012) 192–208.
- [25] I.A. Malik, M. Mirkhalaf, F. Barthelat, Bio-inspired “jigsaw”-like interlocking sutures: modeling, optimization, 3D printing and testing, *J. Mech. Phys. Solids* 102 (2017) 224–238.
- [26] Y. Li, C. Ortiz, M.C. Boyce, Stiffness and strength of suture joints in nature, *Phys. Rev. E* 84 (2011) 062904.
- [27] Y. Li, C. Ortiz, M.C. Boyce, A generalized mechanical model for suture interfaces of arbitrary geometry, *J. Mech. Phys. Solids* 61 (2013) 1144–1167.
- [28] M.S. Hosseini, F.A. Cordisco, P.D. Zavattieri, Analysis of bioinspired non-interlocking geometrically patterned interfaces under predominant mode I loading, *J. Mech. Behav. Biomed. Mater.* 96 (2019) 244–260.
- [29] I.A. Malik, F. Barthelat, Bioinspired sutured materials for strength and toughness: pullout mechanisms and geometric enrichments, *Int. J. Solids Struct.* 138 (2018) 118–133.
- [30] C. Gao, Y. Li, Mechanical model of bio-inspired composites with sutural tessellation, *J. Mech. Phys. Solids* 122 (2019) 190–204.
- [31] N. Lee, L.N. Williams, S. Mun, H. Rhee, R. Prabhu, K.R. Bhattarai, M.F. Horstemeyer, Stress wave mitigation at suture interfaces, *Biomed. Phys. Eng. Express* 3 (2017) 035025.
- [32] E. Lin, Y. Li, J.C. Weaver, C. Ortiz, M.C. Boyce, Tunability and enhancement of mechanical behavior with additively manufactured bio-inspired hierarchical suture interfaces, *J. Mater. Res.* 29 (2014) 1867–1875.
- [33] M. Mirkhalaf, A.K. Dastjerdi, F. Barthelat, Overcoming the brittleness of glass through bio-inspiration and micro-architecture, *Nat. Commun.* 5 (2014) 3166.
- [34] S.M.M. Valashani, F. Barthelat, A laser-engraved glass duplicating the structure, mechanics and performance of natural nacre, *Bioinspiration Biomim.* 10 (2015) 026005.
- [35] B. Lawn, *Fracture of Brittle Solids*, 2nd ed., Cambridge University Press, Cambridge, 1993.
- [36] A. Ziegler, J.C. Idrobo, M.K. Cinibulk, C. Kisielowski, N.D. Browning, R.O. Ritchie, Interface structure and atomic bonding characteristics in silicon nitride ceramics, *Science* 306 (2004) 1768–1770.
- [37] D. Jiao, Z.Q. Liu, R.T. Qu, Z.F. Zhang, Anisotropic mechanical behaviors and their structural dependences of crossed-lamellar structure in a bivalve shell, *Mater. Sci. Eng. C* 59 (2016) 828–837.
- [38] J. Dundurs, Discussion: “Edge-bonded dissimilar orthogonal elastic wedges under normal and shear loading”, *J. Appl. Mech.* 35 (1968) 460–466 *J. Appl. Mech.* 36 (1969) 650–652.
- [39] A.G. Evans, B.J. Dalgleish, M. He, J.W. Hutchinson, On crack path selection and the interface fracture energy in bimaterial systems, *Acta Metall.* 37 (1989) 3249–3254.
- [40] B. Cotterell, J.R. Rice, Slightly curved or kinked cracks, *Int. J. Fract.* 16 (1980) 155–169.
- [41] M.Y. He, J.W. Hutchinson, Crack deflection at an interface between dissimilar elastic materials, *Int. J. Solids Struct.* 25 (1989) 1053–1067.
- [42] K.T. Faber, A.G. Evans, Crack deflection processes – I. theory, *Acta Metall.* 31 (1983) 565–576.
- [43] S. Suresh, Crack deflection: implications for the growth of long and short fatigue cracks, *Metall. Trans. A* 14 (1983) 2375–2385.
- [44] L. Liu, Y. Li, Predicting the mixed-mode I/II spatial damage propagation along 3D-printed soft interfacial layer via a hyperelastic softening model, *J. Mech. Phys. Solids* 116 (2018) 17–32.
- [45] R.O. Ritchie, The conflicts between strength and toughness, *Nat. Mater.* 10 (2011) 817–822.
- [46] M.E. Launey, R.O. Ritchie, On the fracture toughness of advanced materials, *Adv. Mater.* 21 (2009) 2103–2110.
- [47] K. Hayashi, S. Nemat-Nasser, Energy-release rate and crack kinking under combined loading, *J. Appl. Mech.* 48 (1981) 520–524.
- [48] S. Suresh, Fatigue crack deflection and fracture surface contact: micromechanical models, *Metall. Trans. A* 16 (1985) 249–260.